Contribution from the Instituto Tecnológico para la Industria Química (INTEC, CONICET-UNL), Güemes 3450, 3000 Santa Fe, Argentina, Instituto de Física e Química de São Carlos, Universidade de São Paulo, C.P. 369, 13560 São Carlos SP, Brazil, Departmento de Física, Facultad de Ciencias Exactas, Universidad Nacional de La Plata, C.C. 67, 1900 La Plata, Argentina, and Department of Physics, San Diego State University, San Diego, California 92182

Crystal Structure and Magnetic Interactions in Bis(D,L-alaninato)copper(II) Hydrate

R. Calvo,*[1a] P. R. Levstein,†[1a] E. E. Castellano,[1b] S. M. Fabiane,[1b] O. E. Piro,[1c] and S. B. Oseroff[1d]

Received November 21, 1989

The title compound, $Cu(NH_2CHCH_3CO_2)_2 \cdot H_2O$ [Cu(D,L-ala)$_2 \cdot H_2O$], crystallizes in the space group $C2/c$, with $a = 12.087$ (3) Å, $b = 9.583$ (3) Å, $c = 8.973$ (3) Å, $\beta = 110.85$ (2)°, and $Z = 4$. The structure was solved from 737 X-ray reflections and refined to $R = 0.032$. The Cu(II) ion is at an inversion center, bound to the amino nitrogen and to one of the carboxylate oxygens of two symmetry-related (D and L) alanine molecules. Two water oxygens complete an elongated octahedral arrangement of ligands around the copper ions. The water oxygens are at the common apical positions of neighboring coordination octahedra and are strongly hydrogen-bonded to carboxylate oxygens of two other neighboring molecules. The corner sharing octahedra are arranged in chains parallel to $\hat{c}$ at a distance of 4.487 Å, with an interchain distance of 7.712 Å. Magnetic susceptibility data in powdered Cu(D,L-ala)$_2 \cdot H_2O$ between 1.83 and 44 K show, above 10 K, a Curie-Weiss behavior with $\Theta_c = -2.10$ K. The deviation from the Curie-Weiss law observed below Θ_c can be interpreted in terms of a one-dimensional spin chain model, with antiferromagnetic exchange-coupling constant $J/k = -1.61$ K between nearest-neighbor Cu(II) ions. Room-temperature single-crystal EPR data show one exchange-collapsed resonance for all magnetic field orientations and are used to obtain the $\bar{g}$ tensors of individual Cu(D,L-ala)$_2 \cdot H_2O$ molecules. The magnetic coupling between coppers is discussed in terms of the possible paths for superexchange interaction allowed by the lattice, and the results are compared with those obtained from similar studies in other copper amino acid complexes.

Introduction

The study of the electronic properties and magnetic interactions of transition-metal ions in proteins provides information complementary to structural data obtained by X-ray diffraction methods.[2] Exchange interactions between metal ions or between metal ions and free radicals formed during the protein cycle have been observed in biologically relevant proteins.[3] From this connection, it has been suggested that in some cases the magnitude of the superexchange may be used to estimate rates of electron-transfer reactions that occur between magnetic species.[4,5]

Transition-metal derivatives of amino acids constitute model systems for studying electronic properties and magnetic interactions in metalloproteins. They allow one to learn about the properties of the ground orbital state of the magnetic ion and to analyze the role of different amino acid moieties as superexchange paths bridging neighboring metal ions. These circumstances motivated many investigations on their molecular structures,[6] as well as on their electronic and magnetic properties.[7-9] The magnetic properties of copper-amino acid complexes are interesting from other points of view as well. They often crystallize with coppers in layers, giving rise to low-dimensional magnetic behavior, as observed by EPR spectroscopy and magnetic susceptibility measurements.[7-9] The local symmetry and bonding around the copper ions and the magnetic dimensionality of these systems display a wide variety of possibilities by going through the long list of Cu(aa)$_2$ compounds which allow growing of single-crystal samples adequate for structural and magnetic studies. Consequently, they provide useful systems whose behavior can be contrasted against theories on low-dimensional magnetic properties. In this direction, detailed observations of the structural and magnetic properties in series of Cu(aa)$_2$ compounds have led us to determine magnetostructural correlations. Some of these correlations involve changes in the magnetic dimensionality of the system,[10] and some others imply changes in the superexchange path by keeping constant and dimensionality.[11]

Here, a magnetostructural study of the copper complex of the racemic mixture of alanine, Cu(D,L-ala)$_2 \cdot H_2O$, is reported. This investigation was started in order to observe if the interesting trend[10] displayed by other pairs of Cu(L-aa)$_2$ and Cu(D,L-aa)$_2$ was followed by Cu(L-ala)$_2$ and Cu(D,L-ala)$_2$. However, the crystallographic results in Cu(D,L-ala)$_2$ show an arrangement of copper ions completely different from those expected on the basis of the Cu(L-ala)$_2$ structure[12] and the correlations observed in the copper

Table I. Crystal Data, Data Collection Details, and Structure Refinement Results for Cu(D,L-ala)$_2 \cdot H_2O$

formula	$Cu(NH_2CHCH_3CO_2)_2 \cdot H_2O$
mol wt	257.73
space group	$C2/c$ (No. 15)
lattice params	
a	12.087 (3) Å
b	9.583 (3) Å
c	8.973 (3) Å
β	110.85 (2)°
V	971.3 (9) Å^3
Z	4
D(calc)	1.762 g cm^{-3}
sample dimens	0.25 × 0.25 × 0.33 mm
radiation	Mo Kα, $\lambda = 0.71069$ Å
T	25 °C
linear abs coeff (μ)	2.25 mm^{-1}
transm factors (max, min)	0.677, 0.534
scan technique	w-2θ
scan speed range	6.7-20 ° min^{-1}
θ range from data collcd	0-25°
no. ind reflns	845
no. reflns above 3$\sigma(I)$	737
minimized function	$\sum w(\|F_o\| - \|F_c\|)^2$
weighting scheme	$w = 1/\sigma^2(\|F_o\|)$
$R = \sum \|\|F_o\| - \|F_c\|\| / \|F_o\|$	0.032
$R_w = [\sum w(\|F_o\| - \|F_c\|)^2 / w\|F_o\|^2]^{1/2}$	0.033

† Present address: Department of Chemistry, University of Massachusetts, Boston, MA 02125.

(1) (a) Instituto de Desarrollo Tecnológico para la Industria Química (INTEC). (b) Instituto de Física e Química de São Carlos. (c) Universidad Nacional de La Plata. (d) San Diego State University.
(2) Brill, A. S. *Transition Metals in Biochemistry*; Springer Verlag: Berlin, 1977. Gray, H. B.; Solomon E. I. In *Copper Proteins*; Spiro, T. G., Ed.; Wiley: New York, 1981; Chapter 1. Solomon, E. I.; Penfield, K. W.; Wilcox, D. E. In *Structue and Bonding*; Springer: Berlin, 1983; Vol. 53, p 1.
(3) Butler, W. F.; Calvo, R.; Fredkin, D. R.; Isaacson, R. A.; Okamura, M. Y.; Feher, G. *Biophys. J.* **1984**, *53*, 947. Calvo, R.; Passeggi, M. C. G.; Isaacson, R. A.; Okamura, M. Y.; Feher, G. *Biophys. J.* **1990**, *58*, 149.
(4) Okamura, M. Y.; Fredkin, D. R.; Isaacson, R. A., Feher, G. In *Tunneling in Biological Systems*; Chance, B., Ed.; Academic Press: New York, 1979; p 729.
(5) Devault, D. *Quantum Mechanical Tunneling in Biological Systems*; Cambridge University Press: London, 1984.
(6) Freeman, H. C. *Adv. Protein Chem.* **1967**, *22*, 257. Freeman, H. C. In *Inorganic Biochemistry*; Eichhorn, G. L., Ed.; Elsevier: Amsterdam, 1973; Chapter 3.
(7) Newman, P. R.; Imes, J. L.; Cowen, J. A. *Phys. Rev. B* **1976**, *13*, 4093.

0020-1669/91/1330-0216$02.50/0

Table II. Fractional Atomic Coordinates and Equivalent Isotropic Thermal Parameters of Bis(D,L-alaninato)copper(II) Hydrate (Estimated Standard Deviations in Parentheses)[a]

atom	*x/a*	*y/b*	*z/c*	B_{iso}, Å^2
Cu	0	0	0	1.79 (2)
O(1)	0.1100 (2)	0.1304 (2)	0.1478 (2)	2.09 (6)
O(2)	0.2939 (2)	0.2071 (2)	0.2269 (3)	2.72 (6)
C(1)	0.2147 (2)	0.1273 (3)	0.1476 (3)	1.81 (7)
C(2)	0.2394 (3)	0.0217 (3)	0.0336 (4)	2.40 (9)
H(C2)	0.2265	0.0753	−0.0748	5.0
C(3)	0.3636 (3)	−0.0321 (4)	0.0954 (6)	3.8 (1)
H(C3)	0.3918	−0.0955	0.1953	5.0
H′(C3)	0.4273	0.0434	0.1263	5.0
H″(C3)	0.3807	−0.0895	0.0139	5.0
N	0.1470 (2)	−0.0866 (2)	−0.0050 (3)	1.84 (6)
H(N)	0.1666	−0.1467	0.0595	5.0
H′(N)	0.1377	−0.1190	−0.0962	5.0
O(W)	0	−0.1538 (3)	0.25	2.63 (8)
H(OW)	0.0613	−0.2147	0.2681	5.0

[a] Estimated errors of hydrogen parameters are not provided, as they were kept fixed during refinement. See text.

derivatives of L- and D,L-methionine[13,14] and of L- and D,L-aminobutyric acid.[10,15] The path for superexchange between neighboring copper ions in Cu(D,L-ala)$_2$ is different from those observed in other Cu(aa)$_2$. It involves only one nonmagnetic atom (a water oxygen), and the magnitude of the superexchange is consequently larger. Our results are compared to those obtained by Sandreczki et al.[16] in their low-temperature single-crystal NMR studies of Cu(D,L-ala)$_2$·H$_2$O.

Experimental Section

Preparation. The complex was prepared through the reaction of basic copper carbonate added to an aqueous solution of racemic alanine. Unreacted carbonate was removed from the solution by filtering. Deep blue single crystals were grown from saturated water solutions at room temperature. They grow as parallelepipeds of up to 2 × 2 × 3 mm, bounded by (110), (1$\bar{1}$0), and (101) faces and showing [001] and [1$\bar{1}$1] crystal directions.

X-ray Diffraction Data. A complete data set was obtained at room temperature from a six-faceted crystal, by employing an Enraf-Nonius CAD-4 four-circle diffractometer. Experimental details are included in Table I. Diffraction intensities were corrected for Lorentz, polarization, and absorption effects. From the 845 independent reflections measured, 737 having $I > 3\sigma(I)$ were used for the structure determination and refinement. Scattering factors of Stewart et al.[17] for bonded H atoms, atomic scattering factors of Cromer and Waber,[18] and anomalous dispersion coefficients by Cromer and Ibers[18] for the rest of the atoms were used in the calculations. These were performed with the SHELX[19] and SDP[20] systems of programs. The stereoscopic projection given (Figure 2) was drawn with the program ORTEP.[21]

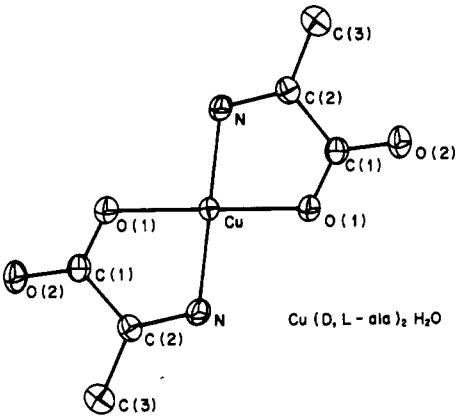

Figure 1. Projection of the copper alanine complex showing the numbering scheme for the non-hydrogen atoms and their thermal vibrational ellipsoids.

Table III. Bond Distances (Å) and Angles (deg) for Cu(D,L-ala)$_2$·H$_2$O

(a) Bond Distances

Cu–O(1)	1.958 (2)	O(2)–C(1)	1.234 (4)
Cu–N	1.976 (3)	C(1)–C(2)	1.542 (4)
Cu–O(W)	2.684 (2)	C(2)–C(3)	1.495 (6)
O(1)–C(1)	1.266 (4)	C(2)–N	1.473 (4)

(b) Bond Angles

O(1)–Cu–N	83.35 (9)	O(2)–C(1)–C(2)	119.7 (3)
O(1)–Cu–O(W)	89.22 (7)	C(1)–C(2)–C(3)	112.7 (3)
N–Cu–O(W)	93.20 (7)	C(1)–C(2)–N	108.0 (3)
Cu–O(1)–C(1)	115.0 (2)	C(3)–C(2)–N	114.9 (3)
O(1)–C(1)–O(2)	123.7 (3)	Cu–N–C(2)	108.1 (2)
O(1)–C(1)–C(2)	116.5 (6)		

(c) Angles around Water Oxygen Atom[a]

Cu–O(W)–Cu′	113.4 (1)
Cu–O(W)–H(OW)	105.00 (4)
Cu–O(W)–H′(OW)	116.40 (3)
H(OW)–O(W)–H′(OW)	100.3 (2)

(d) Distances from Copper to Nearby Protons

Cu–H(N)	2.356	Cu–H(C_3)	4.521
Cu–H′(N)	2.416	Cu–H′(C_3)	4.896
Cu–H(C_2)	3.126	Cu–H″(C_3)	4.639
Cu–O(W)	3.050		

[a] The symmetry operation $-x, y, {}^1/_2 - z$ relates primed and unprimed atoms.

Crystal Structure Determination and Refinement. The crystallographic data for Cu(D,L-ala)$_2$·H$_2$O along with details of the refinement procedure are summarized in Table I. The structure was solved by standard Patterson and Fourier techniques and refined by full-matrix least-squares methods with anisotropic thermal parameters for the non-hydrogen atoms. All hydrogen atoms were located from difference Fourier maps and included at fixed positions in the structure factor calculation, with a common isotropic thermal parameter B = 4.99 Å^2. A list comparing observed and calculated structure factors is available as supplementary material.

Magnetization Measurements. These were performed in powdered samples of Cu(D,L-ala)$_2$·H$_2$O with a VTS 50 squid magnetometer (SHE Corp.) as a function of temperature in the range 1.83–44 K and at a field of 100 G.

EPR Experiments. The EPR spectra were obtained at 9 GHz and room temperature with a Bruker ER-200 spectrometer and a 12-in. rotating electromagnet fitted with a calibrated Hall-probe magnetic field control. A conventional cylindrical microwave cavity with 100-kHz magnetic field modulation was employed.

The single-crystal sample was mounted in an L-shaped orthogonal *xyz* sample holder with the (110) face glued to the *xy* face of the holder, such that its $\hat{x}$ axis was along the [1$\bar{1}$1] crystal direction. The holder was positioned on a horizontal pedestal inside of the cavity. When the magnet was rotated on the horizontal plane, EPR spectra with the magnetic field

(8) Calvo, R.; Mesa, M. A. *Phys. Rev. B* **1983**, *28*, 1244. Calvo, R.; Mesa, M. A.; Oliva, G.; Zuckerman-Schpector, J.; Nascimento, O. R.; Tovar, M.; Arce, R. *J. Chem. Phys.* **1984**, *81*, 4584. Calvo, R.; Isern, H.; Mesa, M. A. *Chem. Phys.* **1985**, *100*, 89.
(9) Gennaro, A. M.; Levstein, P. R.; Steren, C. A.; Calvo, R. *Chem. Phys.* **1987**, *111*, 431. Levstein, P. R.; Steren, C. A.; Gennaro, A. M.; Calvo, R. *Chem. Phys.* **1988**, *120*, 449. Steren, C. A.; Gennaro, A. M.; Levstein, P. R.; Calvo, R. *J. Phys.*: Condens. *Matter* **1989**, *1*, 637.
(10) Levstein, P. R.; Calvo, R.; Piro, O. E.; Rivero, B. E.; Castellano, E. E. *Inorg. Chem.* **1990**, *29*, 3918.
(11) Levstein, P. R.; Calvo, R. *Inorg. Chem.* **1990**, *29*, 1581.
(12) Dijkstra, A. *Acta Crystallorg.* **1966**, *20*, 588.
(13) Ou, C. C.; Powers, D. A.; Thich, J. A.; Felthouse, T. R.; Hendrikson, D. N.; Potenza, J. A.; Schugar, H. J. *Inorg. Chem.* **1978**, *17*, 34.
(14) Veidis, M. V.; Palenik, G. J. *Chem. Commun.* **1969**, 1277.
(15) Fawcett, T. G.; Ushay, M.; Rose, T. P.; Lalancette, R. A.; Potenza, J. A.; Schugar, H. J. *Inorg. Chem.* **1979**, *18*, 327.
(16) Sandreczki, T.; Ondercin, D.; Kreilick, R. W. *J. Am. Chem. Soc.* **1979**, *101*, 2880.
(17) Stewart, R. F.; Davison, E. R.; Simpson, W. T. *J. Chem. Phys.* **1965**, *42*, 3175.
(18) Cromer, D. T.; Waber, J. T. In *International Tables for X-ray Crystallography*; Kynoch Press: Birmingham, England, 1974; Vol IV, p 71. Cromer, D. T.; Ibers, J. A. *Ibid.*; p 149.
(19) Sheldrick, G. M. *SHELX, A Program for Crystal Structure Determination*; University of Cambridge: Cambridge, England, 1976.
(20) Frenz, B. A. *Enraf-Nonius Structure Determination Package*; Enraf-Nonius: Delft, The Netherlands, 1983.
(21) Johnson, C. K. ORTEP. Report ORNL-3794; Oak Ridge National Laboratory: Oak Ridge, TN, 1965.

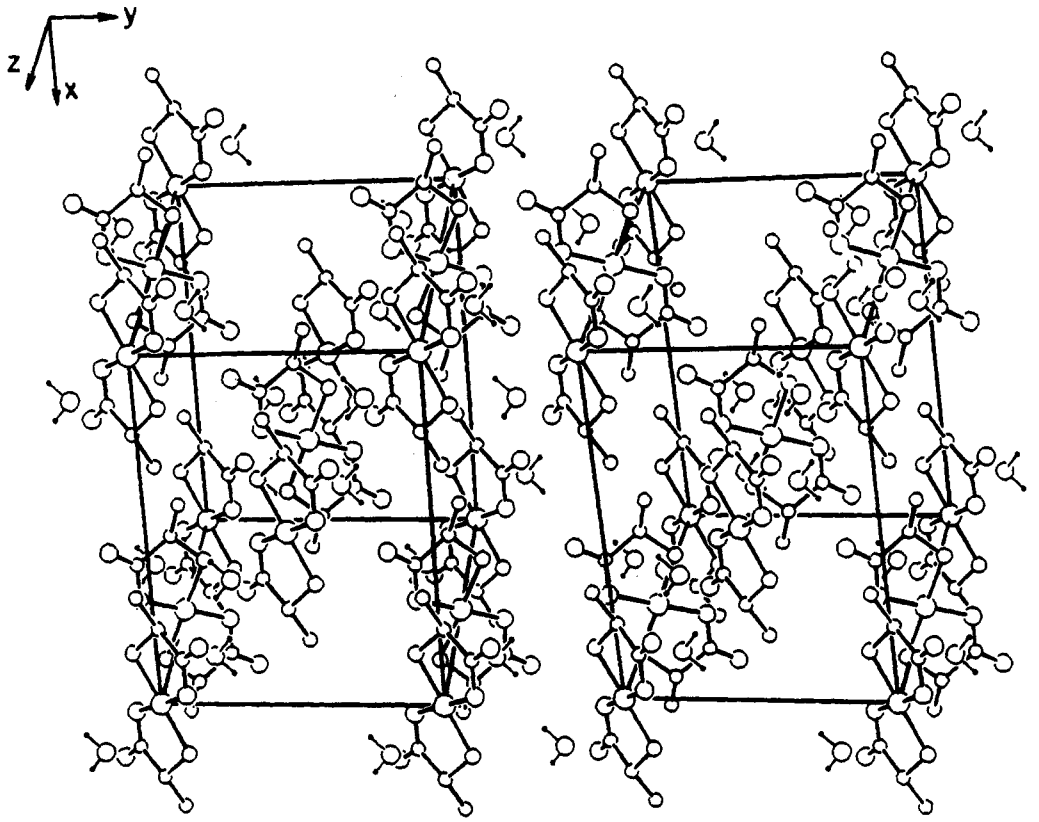

Figure 2. Stereoscopic projection of the $Cu(D,L\text{-ala})_2 \cdot H_2O$ crystal along the $\hat{c}$ axis.

$\vec{H}$ laying on the xy, zx, or zy planes of the sample holder, were recorded at intervals of 15°. The orientation of the crystal $\hat{c}$ axis in the xy plane of the sample holder was determined from the symmetry requirement that the gyromagnetic factor of $Cu(D,L\text{-ala})_2 \cdot H_2O$ should attain an extreme value for $\vec{H} // \hat{c}$.

Results and Discussion

Structural Results. Fractional coordinates and equivalent isotropic temperature parameters[22] for all atoms in $Cu(D,L\text{-ala})_2 \cdot H_2O$ are given in Table II. Relevant interatomic bond distances and angles are in Table III. Figure 1 is a drawing of the copper–amino acid complex showing the labeling of non-hydrogen atoms and their thermal vibration ellipsoids. The parameters of these ellipsoids, along with the ones corresponding to the water oxygen atom, are provided as supplementary material. A stereoscopic view of the crystal packing is shown in Figure 2. The Cu(II) ion, sited on a center of symmetry, is bonded to the oxygen atom [d(Cu–O) = 1.958 (2) Å] and to the nitrogen atom [d(Cu–N) = 1.976 (3) Å] of two symmetry-related D- and L-alanine species, in a crystallographically perfect planar arrangement. Two centrosymmetrically related water oxygen atoms, mounted on a 2-fold symmetry axis, complete the vertices of an elongated octahedron [d(Cu–O(W)) = 2.684 (2) Å] around the copper ion. The water oxygen is at the common vertex of neighboring coordination octahedra, with its electronic lone-pair lobes pointing to (and hence bridging) the corresponding Cu(II) ions. This is emphasized in Figure 3, which shows the octahedron of ligands corresponding to two neighbor copper ions along the $\hat{c}$ axis. The water oxygens are strongly bonded to carboxylate oxygens by hydrogen bridges to two other different neighboring molecules [d(H···O)) = 1.890 (2) Å]. The nearly tetrahedral bonding geometry around the water oxygen in the crystal can be appreciated in Figures 2 and 3 and in the corresponding values of bond angles given in Table IIIc. The molecules are also linked to each other through a net of relatively weak N–H···O hydrogen bonds with carboxylate and bonded-to-copper oxygen atoms. The hydrogen bond structure of $Cu(D,L\text{-ala})_2 \cdot H_2O$ is detailed in Table IV.

(22) Hamilton, W. C. *Acta Crystallogr.* **1959**, *12*, 609.

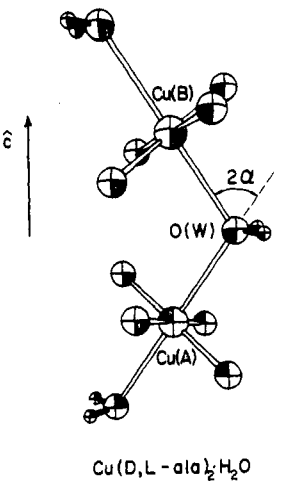

Figure 3. Two neighboring copper ions [labeled Cu(A) and Cu(B)] along the $\hat{c}$ axis, shown together with the octahedra of ligands. The water oxygens, common apical ligands of Cu(A) and Cu(B), provide the shortest possible superexchange path between them. The angle 2α between the symmetry axes of the two octahedra is indicated.

Table IV. Hydrogen Bond Distances (Å) and Angles (deg) for $Cu(D,L\text{-ala})_2 \cdot H_2O$[a]

D	H	A[b]	D···A	H···A[c]	∠D–H···A	D–H
O(W)	H(W)	O(2^i)	2.767 (3)	1.890 (2)	161.0 (1)	0.911 (2)
N	H(N)	O(2^i)	3.062 (3)	2.283 (2)	168.5 (2)	0.791 (2)
N	H′(N)	O(1^{ii})	3.015 (3)	2.203 (2)	161.3 (2)	0.845 (2)

[a] Donor and acceptor atoms are indicated by D and A, respectively. All hydrogen bond interactions with H···A distances up to 2.5 Å are included. [b] Symmetry code: (i) $^1/_2 - x, y - ^1/_2, ^1/_2 - z$; (ii) $x, y, z + ^1/_2$. [c] Standard deviations of distances and angles involving hydrogen atoms (whose positions were not refined; see text) are underestimated, as they were calculated from errors in the corresponding non-hydrogen atom positions only.

Trans coordination of $Cu(D,L\text{-ala})_2 \cdot H_2O$ was proposed earlier by Herlinger et al.[23] on the basis of infrared spectroscopic data

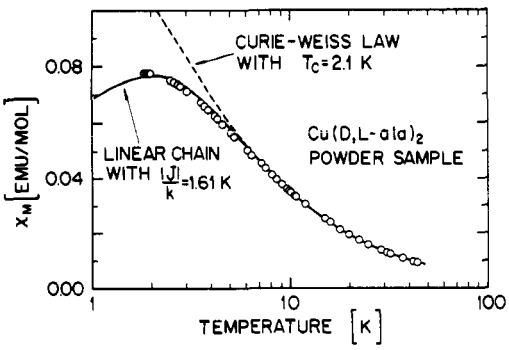

Figure 4. Plot of magnetic susceptibility data $\chi_M(T)$ vs log T emphasizing the departure of the data at low temperatures from the Curie–Weiss behavior. The solid line indicates the $\chi_M(T)$ function calculated by using the model of Bonner and Fisher, as simplified in ref 26, for a spin = $^1/_2$ chain, with an isotropic exchange-coupling constant J/K = −1.61 K. The dashed curve corresponds to the Curie–Weiss law.

for several copper amino acid complexes, in agreement with our structural results.

Sandreczki et al.[16] reported low-temperature proton NMR studies of Cu(D,L-ala)$_2$·H$_2$O single crystals. At low temperatures, when the electronic magnetization is large, the proton resonances are shifted due to dipole–dipole and Fermi contact interactions between the proton spins and the (polarized) electronic spin of the copper ions. The observed angular variation of the NMR shifts allowed those authors to calculate the distances from the copper atoms to the nearby protons. If these results are compared to our more accurate determination of the distances between copper and protons [see Table IIId], small discrepancies (less than 10%) can be detected for the H(C2), H(N), and H′(N) distances to copper, but large differences (up to 30%) occur for the corresponding distances involving the methyl protons. On the basis of our structural data we identify the main source of error in the calculation of distances from NMR data as due to the sizable dipole–dipole couplings of each proton with more than one copper ion. In the case of the water protons which have two neighboring Cu(II) ions (see Figures 2 and 3), Sandreczki et al.[16] were not able to determine the proton–copper distance. This difficulty does not arise when the NMR technique is used to determine proton–metal distances in large molecules, where metal–metal distances are large.

Magnetization Results. The molar susceptibility (χ_M) is plotted in Figure 4 as a function of log T. Above 10 K the data show a well-defined Curie–Weiss behavior[24]

$$\chi_M(T) = C_M/(T - \theta_c) \qquad (1)$$

with antiferromagnetic Curie temperature θ_c = −2.10 K and C_M = 0.427 emu K/mol. Since $C_M = Ng^2\mu_0^2S(S + 1)/3k$,[24] where μ_0 is the Bohr magneton, g the gyromagnetic factor, S the effective spin, and k the Boltzmann constant, we obtain, from a fitting of eq 1 to the high T data, a mean gyromagnetic factor g = 2.135 for the powder sample. Below 10 K the data deviate from the Curie–Weiss law of eq 1. To explain this behavior we used the results of Bonner and Fisher[25] for a chain of $^1/_2$ spins coupled through the Heisenberg (isotropic) exchange interaction.

$$\mathcal{H}_{ex} = -2J\sum_{i=1}^{n}\bar{S}_i\cdot\bar{S}_{i+1} \qquad (2)$$

Numerical calculations by these authors were used by Hatfield and collaborators[26] to propose for the molar susceptibility the following algebraic function

$$\chi_M(T) = (Ng^2\mu_0^2/kT)\frac{^1/_4 + Bx + Cx^2}{1 + Dx + Ex^2 + Fx^3} \qquad (3)$$

where $x = |J|/kT$ and B–F are tabulated constants that accurately fit the results of Bonner and Fisher[25] in the most useful temperature range. By least-squares fitting of eq 3 to our $\chi_M(T)$ data for Cu(D,L-ala)$_2$·H$_2$O, we obtained the magnitude $|J|/k$ = 1.61 K for the exchange interaction between neighboring copper ions along the $\hat{c}$ axis (see Figure 3), defined in eq 2. With this value of J and eq 3 we calculated the $\chi_M(T)$ vs log T indicated by a solid line in Figure 4, where it is compared to the data and to the corresponding curve calculated with the Curie–Weiss law of eq 1, with θ_c = −2.1 K (dashed line). The good agreement between the spin chain model calculation and the data and the absence of a clear phase transition is in favor of a one-dimensional magnetic behavior of Cu(D,L-ala)$_2$·H$_2$O, already suggested by the structural data. Magnetic susceptibility and specific heat data at lower T are needed to give further support to this hypothesis.

According to eq 2 and considering the antiferromagnetic behavior observed at high T, J has to be negative (J/k = −1.61 K). An estimate of J may also be obtained by using the molecular field theory through the relation[24]

$$\theta_c = 2S(S + 1)zJ/3k$$

where z is the number of nearest neighbors of each copper ion. For Cu(D,L-ala)$_2$·H$_2$O we get J/k = −2.1 K, in reasonable agreement with the more accurate result obtained with the spin chain model.

From the temperature dependence of proton lineshift data on Cu(D,L-ala)$_2$·H$_2$O, Sandreczki et al.[16] reported a ferromagnetic Curie–Weiss temperature θ_c = 6.5 K, differing in both sign and magnitude from our θ_c = −2.1 K value. We assign this important difference to the same effects discussed above, when analyzing the proton–copper distances calculated from the NMR lineshifts.

It is interesting to compare the value of J obtained here for Cu(D,L-ala)$_2$·H$_2$O with those collected by Levstein and Calvo[11] for a series of Cu(aa)$_2$ complexes including Cu(L-phe)$_2$, Cu(L-met)$_2$, and Cu(L-leu)$_2$. In Cu(D,L-ala)$_2$·H$_2$O the superexchange path involves two Cu–O(W) bonds (see Figure 3). These bonds have low spin density, as they are practically perpendicular to the equatorial plane of ligands to copper, which contains the d($x^2 - y^2$) orbital state for the unpaired spin. In the case of the Cu(aa)$_2$ complexes analyzed in ref 11, the most important superexchange paths are carboxylate bridges connecting an apical oxygen ligand of one copper to an equatorial ligand of another copper. It was shown[11] that the magnitude of the antiferromagnetic exchange ($J/k \approx -0.3$ K) strongly depends on the copper-to-apical oxygen bond distance, and therefore changes from complex to complex. Our comparison should be completed by considering the magnitude of the exchange in the well-known case of dimeric cupric acetate monohydrate.[24] In that case pairs of copper ions, separated by 2.62 Å, are connected by four symmetry-related bridging carboxylate groups, giving rise to a strong exchange coupling between coppers having $2J$ = −480 K, much larger than that in Cu(D,L-ala)$_2$·H$_2$O and in the carboxylate bridged Cu(aa)$_2$.[11] The complex Cu(L-ala)$_2$, where carboxylate bridges provide exchange paths between coppers with $J \approx -0.5$ K,[27] has a crystal structure[12] very different from that of Cu(D,L-ala)·H$_2$O.

EPR Results. The values of the squared gyromagnetic factor measured as a function of the angle when the magnetic field $\bar{H}$ is applied in the three planes xy, zy, and zx of the sample holder are displayed in Figure 5. The effective spin Hamiltonian

$$\mathcal{H} = \mu_0\bar{H}\cdot\bar{g}\cdot\bar{S} \qquad (4)$$

where μ_0 is the Bohr magneton, $\bar{S}$ the effective spin of copper (S = $^1/_2$), and $\bar{g}$ the gyromagnetic tensor, was used to describe the data. The components of $\bar{g}^2 = \bar{g}\cdot\bar{g}$ in the xyz coordinate system

(23) Herlinger, A. W.; Wenhold, S. L.; Long, T. V. *J. Am. Chem. Soc.* **1970**, *92*, 6474.
(24) Carlin, R. L.; Van Duyneveldt, A. J. *Magnetic Properties of Transition Metals Compounds*; Springer: New York, 1977. Carlin, R. L. *Magnetochemistry*; Springer Verlag: Berlin, 1986.
(25) Bonner, J. C.; Fisher, M. E. *Phys. Rev. A* **1964**, *135*, 640.
(26) Hall, J. W. Ph.D. Dissertation, University of North Carolina, Chapel Hill, NC, 1977. Hatfield, W. E. *J. Appl. Phys.* **1981**, *52*, 1985.
(27) Calvo, R.; Passeggi, M. C. G.; Novak, M. A.; Symko, O. G.; Oseroff, S. B.; Nascimento, O. R.; Terrile, M. C. *Phys. Rev. B.*, in press.

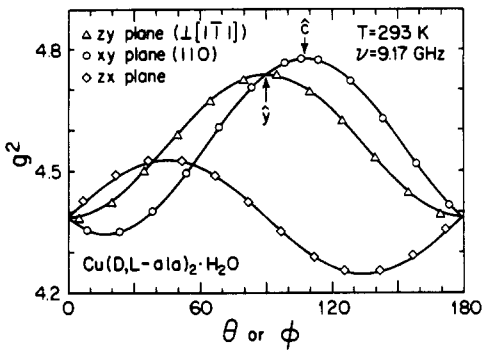

Figure 5. Angular variation of the squared gyromagnetic factor in a single crystal of Cu(D,L-ala)$_2$·H$_2$O. Angles θ and ϕ are defined in the *xyz* system of axes of the sample holder. The sample is positioned in the holder such that its (110) plane is in the *xy* plane, with the [1$\bar{1}$0] direction along the $\hat{x}$ axis. The position of the $\hat{c}$ crystal axis in the *xy* plane is indicated.

were calculated by a least-squares fitting of the data in Figure 5 to the following expresion[8]:

$$g^2(\theta,\phi) = (g^2)_{xx}\sin^2\theta\cos^2\phi + (g^2)_{yy}\sin^2\theta\sin^2\phi + (g^2)_{zz}\cos^2\theta + 2(g^2)_{xy}\sin^2\theta\sin\phi\cos\phi + 2(g^2)_{zx}\sin\theta\cos\theta\cos\phi + 2(g^2)_{zy}\sin\theta\cos\theta\sin\phi \quad (5)$$

where $(g^2)_{ij}$ is the i,j component of the tensor $\bar{g}^2$. This tensor was then diagonalyzed, and the eigenvalues obtained were $(g^2)_1 = 4.781$ (5), $(g^2)_2 = 4.498$ (5), and $(g^2)_3 = 4.230$ (5), corresponding to $\vec{H}$ parallel to the $\hat{c}$, $\hat{b}$, and $\hat{a} = \hat{b} \times \hat{c}$ crystal axes, respectively. The mean gyromagnetic value $g = 2.122$, obtained from the EPR data, agrees well with the value $g = 2.135$ obtained above from the powder susceptibility data. Since there are two magnetically nonequivalent sites for Cu in Cu(D,L-ala)$_2$·H$_2$O [labeled Cu(A) and Cu(B) in Figure 3], having symmetry-related molecular gyromagnetic tensors $\bar{g}_A$ and $\bar{g}_B$, we should expect two EPR resonances for an arbitrary orientation of $\vec{H}$. These two resonances are collapsed into a single line by the exchange interaction coupling the copper ions,[28,29] and consequently, the observed tensor $\bar{g}$ corresponds to a collective resonance having $\bar{g} = {}^1/_2(\bar{g}_A + \bar{g}_B)$.

When the difference between $\bar{g}_A$ and $\bar{g}_B$ is much smaller than the mean gyromagnetic factor $\bar{g}$ it follows that[8]

$$\bar{g}^2 \approx (\bar{g}_A^2 + \bar{g}_B^2)/2 \quad (6)$$

Through eq 6 we can calculate the principal components of the $\bar{g}_A^2$ and $\bar{g}_B^2$ tensors, by making assumptions about their symmetry, and using the eigenvalues of $\bar{g}^2$ given above. The elongated octahedron of ligands to copper in Cu(D,L-ala)$_2$·H$_2$O (see Figure 3) suggests axial symmetry for the $\bar{g}_A$ and $\bar{g}_B$ molecular gyromagnetic tensors, around the line joining the water oxygens. The corresponding principal g values along the O(W)–Cu–O(W) axis ($g_\parallel$) and in the perpendicular plane ($g_\perp$) were determined by the method of Abe and Ono[30] and Billing and Hathaway[31] employing the relations $g_\parallel^2 = (g^2)_1 + (g^2)_2 - (g^2)_3$, $g_\perp^2 = (g^2)_3$, and

$$\cos(2\alpha) = \frac{(g^2)_3 - (g^2)_2}{(g^2)_2 + (g^2)_3 - 2(g^2)_1}$$

where 2α is the angle between the axis of the sites A and B indicated in Figure 3. This procedure leads to $g_\parallel = 2.247$, $g_\perp = 2.057$, and $2\alpha = 69.9°$. These values of $g_\parallel$ and $g_\perp$ are very similar to those observed in other copper–amino acid complexes[7-9] and indicate a $d(x^2-y^2)$ ground orbital for the unpaired electron. The value of 2α determined by EPR agrees well with the value $2\alpha = 72.0°$ between the normals to the corresponding planes of N_2O_2 equatorial ligands obtained from the crystallographic data, hence confirming that the $d(x^2-y^2)$ ground orbital state is in this equatorial plane.

Summary and Conclusions

In the present work we have determined the crystal and molecular structure of Cu(D,L-ala)$_2$·H$_2$O and analyzed its magnetic properties. The molecules are arranged in chains where neighboring Cu(II) ions interact antiferromagnetically through superexchange coupling mediated by a bridging water molecule. This situation is different from those thus far observed in other copper–amino acid compounds, where the superexchange paths are provided by carboxylate bridges[11] or hydrogen bonds.[32] The magnitude of the exchange-coupling constant in Cu(D,L-ala)$_2$·H$_2$O turns out to be several times larger than the corresponding constant obtained in those complexes.

Acknowledgment. This work was supported by Grants 3-098600/88 and 3-907602/85 of Consejo Nacional de Investigaciones Científicas y Tēcnicas (CONICET), Argentina, by Fundação de Amparo a Pesquisa do Estado de São Paulo, Brazil, by Grants RG86-14 of The Third World Academy of Sciences and 11081/1 of Fundaciõn Antorchas. Support from the exchange program between CONICET and CNPq (Brazil) is also gratefully acknowledged.

Supplementary Material Available: A table of anisotropic thermal parameters for the non-hydrogen atoms (Table VI) (1 page); a listing of calculated and observed structure factor amplitudes with their standard deviations (Table V) (5 pages). Ordering information is given on any current masthead page.

(28) Anderson, P. W. *J. Phys. Soc. Jpn.* **1954**, *9*, 316.
(29) Kubo, R.; Tomita, K. *J. Phys. Soc. Jpn.* **1954**, *9*, 888.
(30) Abe, H.; Ono, K. *J. Phys. Soc. Jpn.* **1956**, *11*, 947.
(31) Billing, D. E.; Hathaway, B. J. *J. Chem. Phys.* **1969**, *50*, 1476. Hathaway, B. J.; Billing, D. E. *Coord. Chem. Rev.* **1970**, *5*, 143. See also ref 8.
(32) Hoffmann, S. K.; Goslar, J.; Szczepaniak, L. S. *Phys. Rev. B* **1988**, *37*, 7331.